

**OPTIMIZATION OF THE EARTH REENTRY TRAJECTORY
OF A BLUNTED BODY
BY THE INTEGRAL HEAT FLUX**

V. Yu. Kazakov, S. V. Peigin, and S. V. Timchenko

UDC 533.5:533.6.011

The paper deals with optimization of the Earth reentry trajectory by the magnitude of the total convective heat flux at the stagnation point of a blunted body. The equations of a thin (hypersonic) viscous shock layer taking into account the nonequilibrium nature of chemical reactions and multicomponent diffusion are used as the initial mathematical model for heat flux calculations. The optimal solution is obtained by an effective robust method using the basic ideas of genetic algorithms.

Introduction. As is known, when a body reenters the dense atmospheric layers of the Earth, the heat fluxes to its surface are very great. Therefore, the design of reusable spacecraft involves the complex problem of its thermal protection. In this case, the solution of the problem of decreasing the level of thermal load on spacecraft implies determination of the reentry trajectory and selection of spacecraft design (aerodynamic characteristics, type of heat-protection system, etc.).

The general solution of the complete problem of trajectory optimization by the thermal load on the spacecraft surface reduces to the joint solution of mechanical and gas-dynamic problems. The mechanical problem is the optimal control problem for the ordinary differential equations of motion of a material point in the atmosphere [1–4], which includes aerodynamic coefficients. The gas-dynamic problem includes a calculation of the three-dimensional flow around the entire surface of the spacecraft taking into account physicochemical processes (thermodynamic and chemical nonequilibrium, radiation, etc.), and the aerodynamic coefficients of the first problem are evaluated during solution of the second problem.

Because it is extremely difficult to solve the present problem in a complete joint formulation, extensive use is made of various approximate approaches in which the mechanical and gas-dynamic parts of the problem are separated from each other. For the aerodynamic coefficients, various approximations are employed [2] or these coefficients are treated as parameters of the mechanical problem that permit one to study the so-called reference trajectories. In the optimization problem, depending on the formulation, the integrands for the integer function are approximations along the trajectory for the heat flux to the entire surface of the body or at some points on the body surface (more often, at the stagnation point) [2, 5].

The following parameters were determined in the present paper.

1) The reentry trajectory of a blunted body of specified shape into the Earth's atmosphere along which the total heat flux at the stagnation point of the body has a minimum and the equilibrium temperature of the body surface does not exceed a prescribed value.

2) The trajectory along which the maximum equilibrium temperature of the body surface at the stagnation point is minimal. As the initial gas-dynamic model for determining the heat flux to the body

surface, we use the equations of a thin (hypersonic) viscous shock layer (TVSL) taking into account chemical nonequilibrium and multicomponent diffusion. This model gives high accuracy for altitudes of 100–50 km and velocities of 8–2.5 km/sec [6]. The TVSL equations are solved using a highly effective computational algorithm [7], which is based on a difference scheme of the fourth order of accuracy [8]. The variational problem that arises in determining the optimal trajectory is solved by an effective robust method using the basic ideas of genetic algorithms (GA) [9, 10]. This method employs the principles of evolution and heredity and examines the “population” of possible solutions of the problem that is subjected to the three main “genetic” operators — selection, crossing, and mutation.

Formulation of the Problem. We consider the motion of spacecraft that reenters the Earth’s atmosphere, making the common assumptions for such problems [2]: The Earth is a sphere, the gravitational field is central, the rotation of the Earth is absent, and the atmosphere is immobile. The trajectory lies in the plane of the large circle containing the initial vector (the reentry velocity vector). Variation in the altitude does not lead to marked changes in the gravitational force and centrifugal force. The atmosphere is isothermal, and the density distribution with the altitude is defined by the formula $\rho = \rho_0 \exp(-H/H_m)$, where $H_m = 7.11$ km. The reentry is performed from the orbit of an artificial satellite of the Earth ($V_0 = 7.8$ km/sec), thrust is absent, and the mass of the spacecraft M is constant. In view of this, the equations of motion for atmospheric descent of spacecraft in a moving coordinate system are ordinary differential equations of the third order in time (equations of flight dynamics) for the altitude H , the speed V , the downrange capability L , and the slope of the velocity vector to the plane of the local horizon α under specified initial conditions H_0 , V_0 , L_0 , and α_0 at time t_0 and with controls — the ballistic factor $\sigma(t)$ and the lift-to-drag ratio $K(t)$ [2].

The optimization problem is formulated as follows: to find control functions $\sigma(t)$ and $K(t)$ that provide for a minimum for the functional

$$Q(K, \sigma, t_1) = \min \int_0^{t_1} q(H(t), V(t), R^*, k, k_{wi}, \dots) dt \quad (1)$$

under the constraints

$$|\dot{V}(t)| < ag, \quad T_w < T_w^{\max}. \quad (2)$$

where $q(H(t), V(t), R^*, k, k_{wi}, \dots)$ is the magnitude of the heat flux at the stagnation point on the surface of the spacecraft that moves with speed $V(t)$ at altitude $H(t)$ and has ratio of the principal curvatures k , R^* is the characteristic linear dimension of the body, g is the free-fall acceleration, k_{wi} ($i = 1, \dots, N - 1$) are the known constants of catalytic activity of the surface, and T_w is the equilibrium temperature of the surface at the stagnation point. The constants a and T_w^{\max} are chosen from practical considerations.

The controls $K(t)$ and $\sigma(t)$ are piecewise-smooth functions that are determined by the type of spacecraft (“ballistic” type, “lifting-body” type, “space airplane” type, etc.) and the methods of control (using the ballistic parameter, angles of attack, etc.) [4]. Therefore, the optimization problem (1), (2) should be solved taking into account the particular spacecraft characteristics, which impose limitations on the control law.

The problem of optimization of the spacecraft reentry trajectory by the heat flux can be formulated differently: in the space of continuous functions $V(t)$ and $H(t)$, where $0 \leq t \leq t_1$, it is required to find a pair of functions $V(t)$ and $H(t)$ such that they provide for a minimum for the functional

$$Q(V, H, t_1) = \min \int_0^{t_1} q(H(t), V(t), R^*, k, k_{wi}, \dots) dt \quad (3)$$

under the specified constraints on the maximum acceleration and temperature of the body surface (2).

In problem (2), (3), it is not required to know the design features of particular spacecraft, and, in this sense, it is more general than problem (1), (2). However, additional limitations should be imposed on the range of admissible values to eliminate trivial solutions and solutions that are obviously not integral curves of the flight-dynamics equations [2] and are of no practical interest. The obvious conditions at the boundary points are

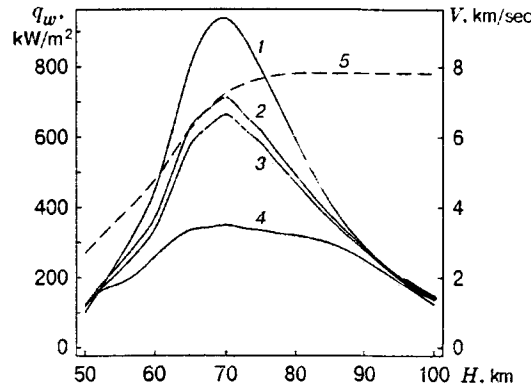


Fig. 1

$$V(0) = V_0, \quad H(0) = H_0, \quad V(t_1) = V^*, \quad H(t_1) = H^*, \quad t_1 \leq t_{\max}. \quad (4)$$

Here the reentry time t_1 is constant or varies from 0 to the maximum reentry time t_{\max} and can be an optimized parameter.

The other additional limitations on the range of admissible values of problem (2), (3) are consequences of the flight-dynamics equations [2]. In particular, it is necessary to impose an additional limitation on the acceleration, i.e., the deceleration cannot be greater than the deceleration caused by the maximum drag force for a given body at a prescribed altitude:

$$|\dot{V}| \leq \frac{S^*}{M} \frac{\rho V^2}{2}. \quad (5)$$

Here S^* is the characteristic region of the spacecraft. Under the very general assumptions on the spacecraft characteristics, the solution of problem (3) subject to constraints (2), (4), and (5) gives a certain trajectory that is possible for an appropriate spacecraft design and suitable methods of control.

Let us now calculate the integrand in (3). As the initial mathematical model for the calculation of the heat flux to the critical point on the body surface, we use the TVSL model. The TVSL equations are the asymptotic forms of Navier–Stokes equations and they describe adequately the flow pattern from the body to the shock wave for $\varepsilon \rightarrow 0$, $\text{Re} \rightarrow \infty$, and $K = \varepsilon \text{Re} \geq O(1)$. Here $\varepsilon = \rho_\infty / \rho^*$ is the ratio of the incident-flow density to the characteristic density in the shock layer and $\text{Re} = VR^* / \mu^*$ is Reynolds number (μ^* is the characteristic viscosity in the shock layer).

A comparison with more accurate models and experimental data shows that, being relatively simple, the TVSL model provides good accuracy (up to 5% for heat fluxes) in the case where the viscous shock layer is thin [6]. These conditions arise for altitudes and velocities that correspond to the upper part of the reentry trajectory in the neighborhood of the critical point of a smooth blunted body.

The heat flux to the stagnation point is defined by

$$q(H(t), V(t), R^*, k, k_{wi}, \dots) = 0.5 \rho V^3 X_q(H(t), V(t), R^*, k, k_{wi}, \dots). \quad (6)$$

Here X_q is the dimensionless heat flux to the surface, which is determined by numerical solution of the TVSL equations taking into account nonequilibrium chemical reactions in air, multicomponent diffusion, and heterogeneous catalytic reactions [7]. As the conditions on the boundary of the body for the energy equation, we use the balance relation for the equilibrium temperature.

The convective heat flux to the critical point of a blunted body is usually determined from the Fay–Riddell formula [11, 12], which is obtained by approximation of numerical calculations of the laminar boundary layer near an ideally catalytic surface with equilibrium chemical reactions. In this case, the analytic nature of the integrand makes the solution of the optimization problem much simpler. However, the maximum heat fluxes at the stagnation point fall in the region of the gliding trajectory at altitudes of 80–65 km, where the Reynolds numbers are relatively small and the chemical reactions are of a strongly nonequilibrium nature [6].

Figure 1 shows the heat fluxes to the critical point of a sphere with $R^* = 0.5$ m obtained for an ideally catalytic surface (curves 1–3) and a noncatalytic surface (curve 4) at $T_w = 1200$ K (curves 1 and 2) and for the case of equilibrium surface temperature (curves 3 and 4) using the Fay–Riddell formula (curve 1) and numerical solution of the TVSL equations (curves 2–4) for the trajectory of [13] (curve 5 is the speed along the trajectory). A comparison of curves 1 and 2 shows that calculations using the Fay–Riddell formula give an error of up to 40% on the most heat-loaded segment of the trajectory.

Method of Solution. To solve the optimization problem (3) subject to constraints (2), (4), and (5) we employ the method of [9, 10], which includes deterministic and probabilistic approaches and uses the main ideas of genetic algorithms [14–16]. The latter are search algorithms based on the mechanisms of natural selection and genetics. They combine natural selection among string structures with partly ordered exchange of information. Being probabilistic, genetic algorithms are nevertheless not a version of random search because here the previously obtained information is effectively used in selection of new points with optimal properties.

These algorithms are iterative. In iteration t (generation t), an ordered set $P(t) = \{x_1^t, \dots, x_n^t\}$ is considered (population of individuals). Each individual (potential solution of the problem) is shown in a certain, possibly rather complex, data structure S . Each solution x_i^t is evaluated, and the measure of its suitability is determined. Next, a new population (iteration or generation $t + 1$) is formed.

At the first step of this formation (step of selection) there is selection of individuals possessing the best qualities. At the next step, some of the selected individuals are transformed by “genetic operators” — mutation and crossing. The mutation operator m_i generates a new individual by a relatively small change in one individual ($m_i: S \rightarrow S$), and the crossing operator c_j performs stronger transformations and generates a new individual by combining parts from several (two or more) individuals ($c_j: S \cdots S \rightarrow S$). After a number of iterative steps, the algorithm converges to the best of the possible solutions.

An important feature of genetic algorithms is their robustness: they converge to a global optimum, which is important for problems whose integer function has local extrema. In contrast to the classical gradient methods of optimization, genetic algorithms do not require strong limitations on the smoothness of the integer function and allow one to find an optimum even for the case of a discontinuous integer function.

Genetic algorithms, proposed at the end of 1960s and substantiated theoretically in 1975 [14], have been widely used (by virtue of their universality and high effectiveness) to solve search and optimization problems in various fields of science and engineering [15].

To solve the above problem, we use a version of the “material” genetic algorithm in which the data structure S is a set of strings of finite length, whose components are real numbers.

The required functions $V(t)$ and $H(t)$ are sought in the class of Besier splines of the m th order, which are expressed in terms of Bernshtein polynomials $B_i^m(t)$:

$$R(\tau) = \sum_{i=0}^m B_i^m(\tau) P_i, \quad B_i^m(\tau) = C_m^i \left(\frac{\tau}{\tau_1} \right)^i \left(1 - \frac{\tau}{\tau_1} \right)^{m-i}, \quad C_m^i = \frac{m!}{i!(m-i)!},$$

$$R(\tau) = \{H(\tau), V(\tau)\}, \quad P_i = \{H_i, V_i\}, \quad i = 0, \dots, m, \quad 0 \leq \tau \leq \tau_1.$$

Here $\tau = t/t^*$ is dimensionless time, t^* is the characteristic time, and P_i are the coordinates of the control points. The Besier curve is defined by the coordinates (H_i, V_i) of the points P_i and the dimensionless reentry time τ_1 .

In our case, the first point $P_0 = (H_0, V_0)$ and last point $P_m = (H^*, V^*)$ are fixed, and this corresponds to conditions (4). Thus, the string $S = (a_1, a_2, \dots, a_{2m-1})$, where

$$a_i = H_i, \quad 1 \leq i \leq m-1; \quad a_i = V_{i-m+1}, \quad m \leq i \leq 2(m-1); \quad a_{2m-1} = \tau_1$$

defines the reentry trajectory in the class of Besier splines of the m th order. According to GA, the set S is a chromosome and its element a_i is a gene. In this case, a_i vary from the lower bound \min_i to the upper bound \max_i . To take into account the constraints on the admissible solutions (2), (5) in the algorithm for searching for the optimal solution (3), we used the modified integer function

$$Q^* = \begin{cases} q_1 + q_2(|\dot{V}(t)|/g - a), & |\dot{V}(t)| > ag, \\ q_3 + q_4(T_w^{\max} - T_w)/T_w^{\max}, & T_w > T_w^{\max}, \\ q_5 + q_6(|\dot{V}(t)|/g - S^*\rho(t)V^2(t)/(2Mg)), & |\dot{V}(t)| > S^*\rho(t)V^2(t)/(2M), \\ Q, & \text{otherwise.} \end{cases}$$

The coefficients q_i ($i = 1, \dots, 6$) were selected so that with violation of any of the constraints, the value of the modified integer function Q^* was obviously larger than Q . In addition, by choosing q_i , it is possible to control the relative significance of the constraints. This approach allows one to extend the range of search of the solution and to evaluate the integer function with violation of the constraints.

Thus, the method includes the following algorithmic steps:

1. The initial flight paths are selected in a random fashion, and the initial "population" $P(0) = \{S_1 \dots S_{N_p}\}$, consisting of N_p individuals, is determined. Next, the integer function Q^* is evaluated for each individual S_k .

2. At the first step of formation of the next generation (selection), we select individuals that possess the best suitability. Tournament selection is used [15]. Sequentially, from two neighboring elements S_i and S_{i+1} ($i = 1, 3, \dots$) of the current population P , the element with the smallest value of Q^* is selected and placed in the intermediate population P' . After the first run (only half the population P' has been formed), the initial population is mixed and the second half of the intermediate population is formed in a similar manner.

3. All sequential pairs of elements from P' are subjected to crossing (with probability p_s) or remain unchanged. The mechanism of simple single-point crossing for the material GA is as follows. Let $A_1 = (y_1, y_2, y_3, y_4)$ and $A_2 = (y'_1, y'_2, y'_3, y'_4)$ be the "parents" chosen during selection. The point of section is found in a random fashion, and the "parents" generate two "descendants" $B_1 = (y_1, y'_2, y'_3, y'_4)$ and $B_2 = (y'_1, y_2, y_3, y_4)$ (the point of section is located after the first gene). After this, the "children" are "substituted" for the "parents" in the intermediate population P' .

4. All elements of the intermediate population P' are subjected to mutations (with probability p_m). We use the inhomogeneous mutation determined by Mikhalewicz [17]. If a gene y_i undergoes mutation, its new changed value y'_i is selected in a random fashion within the interval $[\min_i, \max_i]$:

$$y'_i = \begin{cases} y_i + s(\max_i - y_i)(1 - l/L)^b, & \text{round}(s') = 0, \\ y_i + s(\min_i - y_i)(1 - l/L)^b, & \text{round}(s') = 1. \end{cases}$$

Here s and s' are random numbers from the interval $[0, 1]$, $\text{round}(\cdot)$ is a rounding function, l is the generation number, L is the maximum number of generations, b is a refinement parameter, and \min_i and \max_i are the lower and upper boundaries of variation in the value of the variable y_i . In implementation of GA (evolution), this adaptive mutation allows us to obey the necessary balance between two different-scale changes (mutations) of genes since at the initial steps of the algorithm, large-scale changes (ensuring a broad search area) dominate, and at the final step there is a refinement of the solution (by decreasing the scale of mutations). The refinement parameter b depends on the nature of convergence of the iterative process [9]. After attainment of a stationary state in which the best of the individuals did not change during the last p generations, the value of b is decreased twice, which extends the search area and eliminates the traps of local extrema.

To eliminate premature (false) convergence, we use the approach of [9], in which the probability of mutation of the "descendant" depends on how close the "parents" are among themselves.

For quantitative evaluation of the closeness of the individuals $A = (a_1, \dots, a_i, \dots, a_n)$ and $B = (b_1, \dots, b_i, \dots, b_n)$ selected for crossing, we use the relative distance between them:

$$\text{dist}(A, B) = \frac{1}{n} \sum_{i=1}^n \left(\frac{a_i - b_i}{\max_i - \min_i} \right)^d,$$

where d is a parameter of the problem. Then, the probability of mutation $p_m(A, B)$ is defined by

$$p_m(A, B) = p_d(1 - \text{dist}(A, B)),$$

where p_d corresponds to the maximum permissible probability of mutation. In the calculations, we set $d = p_d = 0.2$.

5. After completion of mutation, values of the integer function Q^* are calculated for the entire population P' , and then one of the elements P' is replaced in a random fashion by the best individual from the previous generation P (elitism). After that the generation P is completely replaced by the generation P' .

6. If the difference of the integer function inside the current generation is smaller than the prescribed value of δ , the process is completed. Otherwise, it is repeated from step 2.

The method was tested on special test integer functions [9, 15], which, besides a global minimum, have a great number of local extrema. For example, for the Rosenbrook function

$$f(x) = 100(x_1^2 - x_2)^2 + (1 - x_1)^2 \quad (-2.048 \leq x_i \leq 2.048)$$

the employed version of GA converged to a global minimum in 96% of 1000 runs with a mean number of generations of about 2000 in one run. An analysis of the solutions for the test functions indicates the high convergence, efficiency, and universality of the present method.

Since GA are based on a probabilistic, nondeterministic approach, a solution can be obtained only in the presence of a sufficient number of runs of the problem. However, even a single run gives information on the characteristics of the optimal solution. In the present work, we performed not less than 10 runs for each version. This allows us to state that the solution belongs to the confidence interval.

The integral in the integer function (3) was calculated by an adaptive algorithm based on the Newton-Cotes formula of the eighth order [19]. As a result, the specified accuracy was attained at a minimum of calculations of the integrand. On the average, 30 calculations of the heat flux along the trajectory are required to reach an error of 10^{-5} . The total number of calculations of the integer function is equal to $N_c = N_p N_g$, where $N_p = 20$ is the number of individuals in the population and $N_g = 2000-4000$ is the number of generations required to achieve the specified accuracy.

Since N_c is large, a direct calculation of the heat flux in (3) by numerical solution of the TVSL equations required large computing costs even in the presence of a highly effective algorithm. Therefore, along with the exact solution of the problem, we used a two-step approach to the heat flux calculation. At the first step, we calculated the TVSL equations for specified values of the determining parameters of the problem R^* , k , and k_{wi} using the algorithm of [7] on a 21×22 grid with a step $\Delta V_\infty = 0.25$ km/sec in the speed range 7.8–2.3 km/sec and with a step $\Delta H = 2.5$ km in the altitude range 100–50 km. At the second step, the integer function (3) was calculated by interpolation of the heat flux data using B -spline surfaces of the sixth order.

The difference between magnitudes of the total heat flux along different trajectories obtained by accurate calculations and the approximate approach described above is not larger than 0.5%, which allows the approximate approach to be used in series calculations. It should be noted that, providing high accuracy, this approach, on the one hand, takes into account the dependence of the heat flux on the main determining parameters of the problem, and, on the other hand, it accelerates sharply the work of GA on search for the optimal solution.

Calculation Results. The results presented here were obtained for ideally catalytic surfaces and non-catalytic surfaces and in the neighborhood of bluntness for the following values of the determining parameters for characteristic dimensions $R^* = 0.5$ and 1.0 m.:

$$S^*/M = 2.5 \cdot 10^{-3} \text{ m}^2/\text{kg}, \quad a = 3.0, \quad T_w^{\max} = 1500 \text{ and } 2500 \text{ K}, \quad k = 0.4 \text{ and } 1.0,$$

$$t^* = 60 \text{ sec}, \quad V_0 = 7.8 \text{ km/sec}, \quad V^* = 2.7 \text{ km/sec}, \quad H_0 = 100 \text{ km}, \quad H^* = 50 \text{ km}.$$

Versions with fixed reentry time τ_1 were considered. Constraints (4) and (5) were always taken into account. We note that the constraint on maximum deceleration (5) is stronger than the constraint on overload (2). Therefore, for the given determining parameters of the problem, constraint (2) was satisfied automatically.

TABLE 1

Version No.	R^* , m	Surface type	$q_w(H_0, V_0)$, W/m ²	S^*/M , m ² /kg	k
1	1.0	Ideally catalytic	98 546.1	$2.5 \cdot 10^{-3}$	1.0
2	1.0	Noncatalytic	94 113.8	$2.5 \cdot 10^{-3}$	1.0
3	0.5	Noncatalytic	122 549.7	$2.5 \cdot 10^{-3}$	1.0
4	1.0	Noncatalytic	91 113.8	$2.5 \cdot 10^{-2}$	1.0
5	1.0	Ideally catalytic	98 546.1	$2.5 \cdot 10^{-2}$	1.0
6	0.5	Noncatalytic	122 549.7	$2.5 \cdot 10^{-2}$	1.0
7	1.0	Noncatalytic	77 919.2	$2.5 \cdot 10^{-3}$	0.4

TABLE 2

Version No.	T_w^{\max} , K	\bar{Q}				T^* , K			
		$\tau_1 = 5$	$\tau_1 = 10$	$\tau_1 = 20$	$\tau_1 = 30$	$\tau_1 = 5$	$\tau_1 = 10$	$\tau_1 = 20$	$\tau_1 = 30$
1	2500	18.24	26.56	38.01	47.04	1900	1783	1706	1618
1	1500	19.02*	31.03*	47.33*	59.60	1860*	1682*	1527*	1494
2	2500	11.06	16.78	25.10	33.52	1585	1487	1427	1388
2	1500	11.24*	16.78	25.10	33.52	1555*	1487	1427	1388
3	2500	12.67	20.09	30.61	41.86	1737	1667	1613	1588
3	1500	13.44*	23.43*	42.51*	58.55*	1712*	1604*	1555*	1530*
4	2500	5.20	8.28	12.40	16.18	1360	1329	1327	1297

* Trajectories with limitation $T_w \leq T_w^{\max} = 1500$ K do not exist. The data are given for the trajectory with minimum equilibrium temperature of the surface.

Since the equilibrium temperature of the body surface T_w depends on the characteristic linear dimension of the problem and the catalytic activity of the surface, for rather low values of T_w^{\max} , the initial problem of choosing the optimal trajectory may not have a solution because it is impossible to satisfy the constraint (2) on the maximum equilibrium temperature of the surface. Therefore, in the case where the problem of finding the trajectory with minimum total heat flux with limitation on the maximum equilibrium temperature of the surface (trajectory with minimum thermal load) had no solution, we posed and solved the problem of finding the trajectory along which the maximum value of the equilibrium temperature of the body surface at the stagnation point had a minimum (trajectory with minimum equilibrium temperature).

Results of the calculations performed are shown in Tables 1 and 2 and Figs. 2-5. Table 1 gives values of the determining parameters of the problem for seven basic versions of calculation. For some of these versions, Table 2 gives relative values of the integer function $\bar{Q} = Q/(q_w(H_0, V_0) \cdot 1 \text{ sec})$ and maximum values of the surface temperature T^* along the optimal trajectory. The data are presented for the best of 10 runs in each version. About 4000 generations are required to reach similarity between individuals with an error of 10^{-7} .

In Figs. 2-4, the results obtained for version Nos. 1, 2, 3, and 7 (Table 1) are indicated by triangles, crosses, circles, and squares, respectively. The solid curves correspond to $T_w^{\max} = 2500$ K and the dashed curves correspond to $T_w^{\max} = 1500$ K.

Figure 2a and b shows curves of $H/H_0(\tau)$ (curves 1) and $V/V_0(\tau)$ (curves 2) obtained for reentry times $\tau_1 = 5$ and 10, respectively, and Figs. 3 and 4 show the equilibrium temperature of the surface $T_w(\tau)$ and the relative acceleration $\dot{V}/g(\tau)$ for reentry time $\tau_1 = 10$.

We note that although the total thermal load \bar{Q} (Table 2) and the equilibrium temperature of the surface T_w (Table 2; Fig. 3) depend on the characteristic dimension of the body, the ratio of the principal curvatures, and the catalytic properties of the surface, the trajectories of minimum thermal load (see Fig. 2) obtained at $T_w^{\max} = 2500$ K (solid curves) practically coincide for all versions and all reentry times considered. Indeed, the heat-flux distributions along the trajectory are qualitatively identical. Minimum heat fluxes occur at the extreme points of the trajectory: at the top, where the incident-flow density ρ_∞ is minimal, and at the

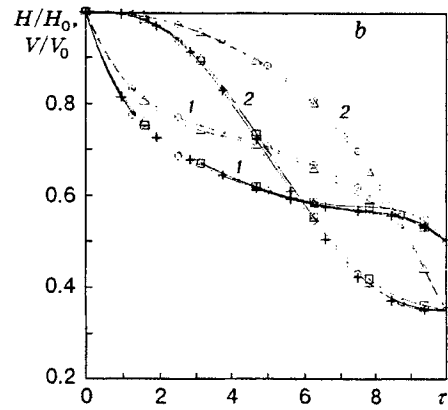
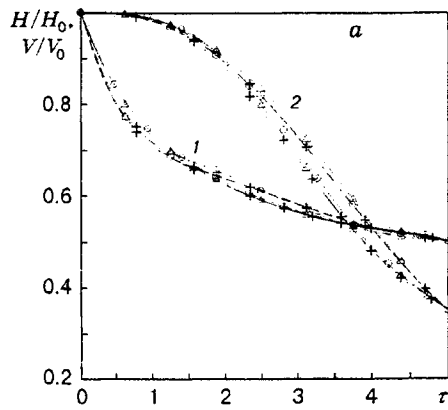


Fig. 2

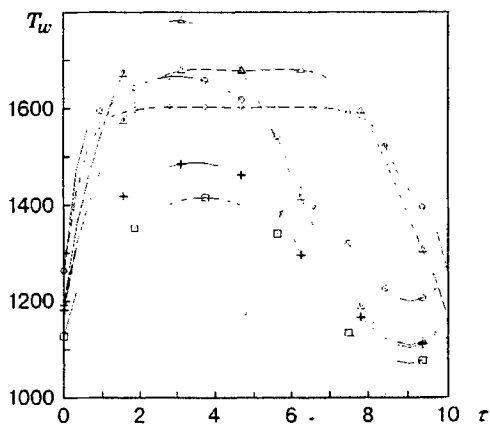


Fig. 3

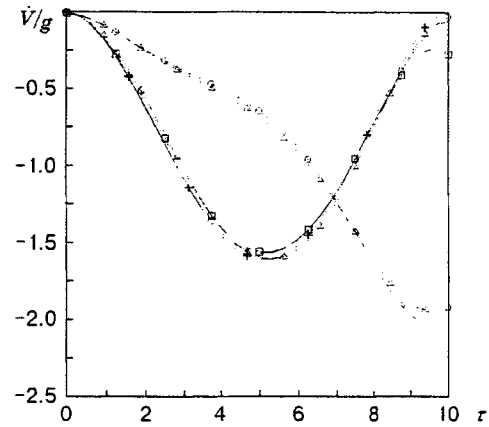


Fig. 4

bottom, where the speed V_∞ is minimal. Therefore, the trajectory of minimum thermal load is constructed so that the maximum larger portion of the load is in the regions of low densities and low velocities. However, the constraint on maximum deceleration (5) does not permit one to decrease the speed at high altitudes. Therefore, on the first segment of the trajectory, maximum deceleration develops (Fig. 4), and on the second segment there is motion with a nearly minimum speed. The dimensions of these segments are determined by the value of τ_1 .

The presence of the local maximum of altitude at the second segment of the trajectory also results from the optimal trajectory (solution) tending to low densities at minimum velocities. This is confirmed by the calculation results given in Fig. 5, which shows curves of $H/H_0(\tau)$ (curves 1) and $V/V_0(\tau)$ (curves 2) for the basic version Nos. 4-6 (see Table 1) at $\tau_1 = 10$ and $T_w^{\max} = 2500$ K (crosses, triangles, and circles in Fig. 5, respectively). It is evident that an increase in S^*/M allows one to attain minimum velocities at high altitudes, which leads to a considerable decrease in thermal load in the neighborhood of the critical point of the body and to a decrease in the surface temperature.

Thus, in the absence of the constraint on the equilibrium surface temperature T_w , the shape of the trajectory with minimum thermal load is determined primarily by the aerodynamic characteristics of the spacecraft (ratio S^*/M) and the reentry time τ_1 . The total thermal load \bar{Q} and the equilibrium temperature on the surface for the present trajectory depend on the characteristic dimension R^* of the body, the ratio of the principal curvatures, the catalytic properties of the surface, and the aerodynamic properties of the body.

The trajectories with minimum local temperature of the surface (dashed curves in Fig. 2) differ significantly from the trajectories of minimum thermal load. Their shapes depend on both the characteristic

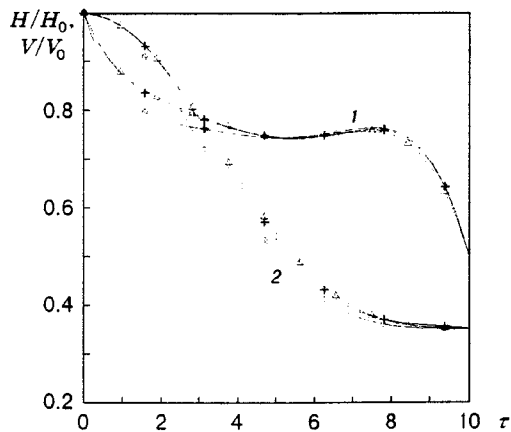


Fig. 5

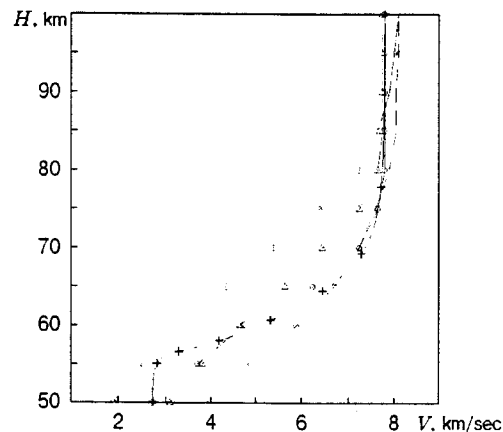


Fig. 6

dimension of the problem and the catalytic properties of the surface. Although the maximum surface temperature for these trajectories is lower than the corresponding value for the minimum thermal load trajectories (dashed curves in Fig. 3), the integral heat flux for them is greater than that for the minimum thermal load trajectories.

In conclusion, we compare the optimal trajectory of minimum thermal load obtained in the present work with some other well-known trajectories. Figure 6 shows quasistationary trajectories with gliding coefficients of 10^{-3} and $2 \cdot 10^{-4} \text{ m}^2/\text{N}$ [3] (solid and dashed curves with rhombuses, respectively), the optimal trajectory obtained in the present work and corresponding to the second version (see Table 1) for $\tau_1 = 10$ and $T_w^{\text{max}} = 1500 \text{ K}$ (crosses), the "Space Shuttle" trajectory [13] (triangles), and the "Buran" trajectory [20] (circles). It is evident that the optimal trajectory computed in the present work correlates well with the "Buran" trajectory in the altitude range $H = 100\text{--}60 \text{ km}$ (segment of maximum thermal loads).

This work was supported by the Russian Foundation for Fundamental Research (Grant No. 98-01-00298).

REFERENCES

1. J. Martin, *Atmospheric Reentry. An Introduction to Its Science and Engineering*, Prentice-Hall, Englewood Cliffs, New Jersey (1968).
2. V. V. Andrievskii, *Dynamics of Earth Reentry of Spacecraft* [in Russian], Mashinostroenie, Moscow (1970).
3. L. M. Shakdov, R. S. Bukhanova, V. F. Illarionov, and V. P. Plokhikh, *Mechanics of Optimal Spatial Motion of Spacecraft in the Atmosphere* [in Russian], Mashinostroenie, Moscow (1972).
4. N. M. Ivanov and A. I. Martynov, *Motion of Spacecraft in the Atmospheres of the Planets* [in Russian], Nauka, Moscow (1985).
5. M. A. Argunchitseva and N. N. Pilyugin, *Extremal Problems of Radiation Gas Dynamics* [in Russian], Izd. Mosk. Univ., Moscow (1997).
6. S. V. Peigin and G. A. Tirskii, "Three-dimensional problems of super- and hypersonic flows of a viscous gas past bodies," *Itogi Nauki Tekhniki. Ser. Mekh. Zhidk. Gaza*, **22**, VINITI, Moscow (1988), pp. 62-177.
7. V. Yu. Kazakov and S. V. Peigin, "Spatial multicomponent viscous shock layer on a catalytic surface in the neighborhood of the critical point," *Teplofiz. Vys. Temp.*, **26**, No. 5, 901-908 (1988).
8. I. V. Petukhov, "Numerical calculation of two-dimensional flows in the boundary layer," in: *Numerical Methods of Solving Differential and Integral Equations and Quadrature Formulas* [in Russian], Nauka, Moscow (1964), pp. 304-325.
9. M. Sefioui, J. Periaux and J.-G. Ganascia, "Fast convergence thanks to diversity," in: *Proc. 5th Annu. Conf. on Evolutionary Programming*, MIT Press, Cambridge (1996).

10. S. V. Peigin, J. Perio, and S. V. Timchenko, "Use of genetic algorithms to optimize the shape of a body by the heat flux," *Mat. Model.*, **10**, No. 9, 111–122 (1998).
11. J. A. Fay and F. R. Riddell, "Theory of stagnation point heat transfer in dissociated air," *J. Aeronaut. Sci.*, **2**, 73–85 (1958).
12. V. P. Agafonov, V. K. Vertushkin, A. A. Gladkov, and O. Yu. Polyanskii, *Nonequilibrium Physicochemical Processes in Aerodynamics* [in Russian], Mashinostroenie, Moscow (1972).
13. R. V. Masek, D. Hender, and J. A. Forney, "Evaluation of aerodynamic uncertainties for the 'Space Shuttle'," AIAA Paper No. 737 (1973).
14. J. H. Holland, *Adaptation in Natural and Artificial Systems*, Univ. Michigan Press, Ann Arbor (1975).
15. D. E. Goldberg, *Genetic Algorithms in Search, Optimization, and Machine Learning*, Addison-Wesley, New York (1989).
16. F. Hoffmeister and T. Back, "Genetic algorithms and evolution strategies: similarities and differences," in: *Parallel Problem Solving from Nature*, Proc. of the 1st Workshop (Dortmund, Germany, October 1–3, 1991), Dortmund (1991), pp. 455–469.
17. Z. Michalewicz, *Genetic Algorithms + Data Structures = Evolution Programs*, Springer-Verlag, New York (1992).
18. K. A. DeYong, "Analysis of behavior of a class of genetic systems," PhD Thesis, Univ. Michigan Press, Ann Arbor (1975).
19. G. E. Forsythe, M. A. Malcolm, and C. B. Moler, *Computer Methods for Mathematical Computations*, Prentice-Hall, Englewood Cliffs, New Jersey (1977).
20. G. E. Lozino-Lozinskii, "Flight of 'Buran'," in: *Gagarin Readings on Astronautics and Aviation, 1989* [in Russian], Nauka, Moscow (1990), pp. 6–21.